6 Results

The results are presented in the following order:

- **Sections 6.1 – 6.3**: The TCR chains identified in the CD8+ T cell clone UZ3/4 are described and the data that specify their involvement in the cross-recognition of mycobacterial and murine hsp60 peptides are shown.
- **Sections 6.4 – 6.5**: The generation of TCR transgenic mice specific for these peptides is summarized and preliminary data from these mice are presented.
- **Section 6.6**: The potential of the mycobacterial hsp60 peptide to induce a CD8+ T cell response to BCG infection is demonstrated.
- **Sections 6.7 – 6.11**: The discovery of the unexpected phenotype of TCR a 7.2 transgenic mice, namely increased frequency of CD4+ TCR $\alpha^{-}\beta^{+}$ T cells causing exaggerated development of IBD, is reported and data suggesting a mechanism for this phenomenon are given.

6.1 Expression of two TCR alpha chains in the CD8+ T cell clone UZ3/4

In order to analyze the TCR composition of the hsp60 specific CD8+ T cell clone UZ3/4, mRNA was prepared from cultured UZ3/4 T cell clone cells. TCR α and β cDNA was PCR- amplified by performing 5'- rapid amplification of cDNA ends (RACE) (Frohman et al., 1988), sequenced and identified by BLAST database search (Pecorari et al., 1999). Two successfully in-frame rearranged TCR α chain genes and one TCR β chain gene were identified. The β chain rearrangement was Vβ8.1–Dβ1–Jβ1.1, the α loci rearrangements were Vα7.2-J18 and Vα8.2-J42, subsequently referred to as TCR β8, TCR α7 and TCR α8 (**Figure 10**). TCR genes were PCR-

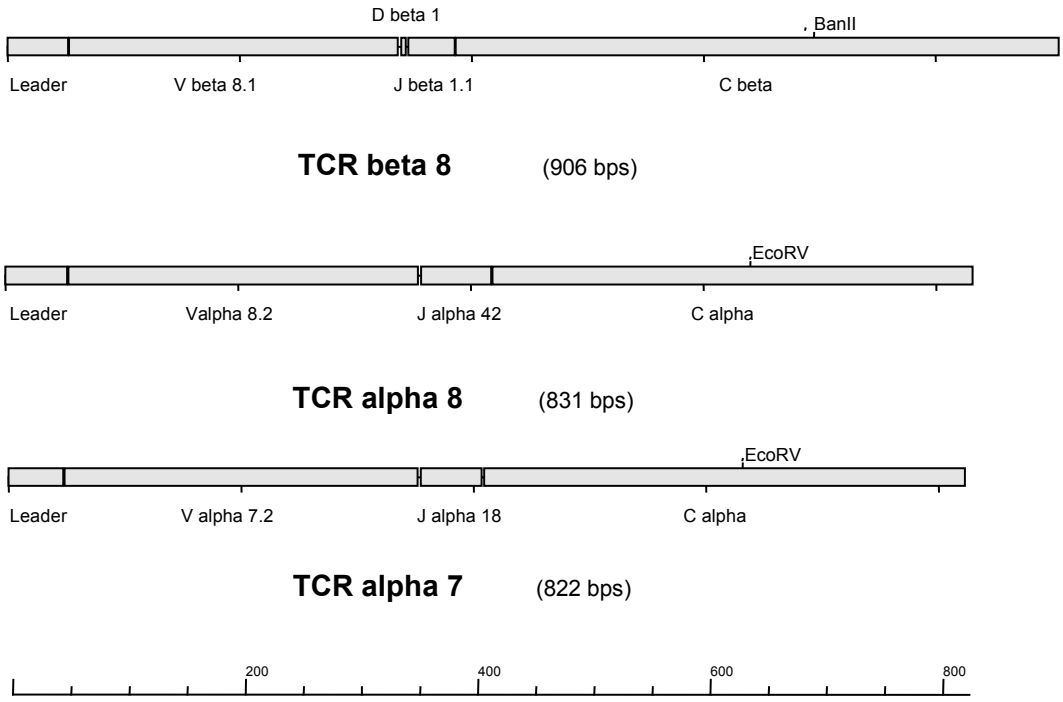

Figure 10. The CD8+ T cell clone UZ3/4 has 3 rearranged TCR chains. Schematic representation of cDNA from TCR β8, TCR α8 and TCR α7. Gray bars correspond to TCR gene segment composition and relative size. Scale indicating the number of base pairs. The marked natural restriction sites BanII and EcoRV were used to subclone the rearranged TCR genes into the plasmids pP142β8AR and pP14α2AR, respectively. The scale represents basepairs (bps).

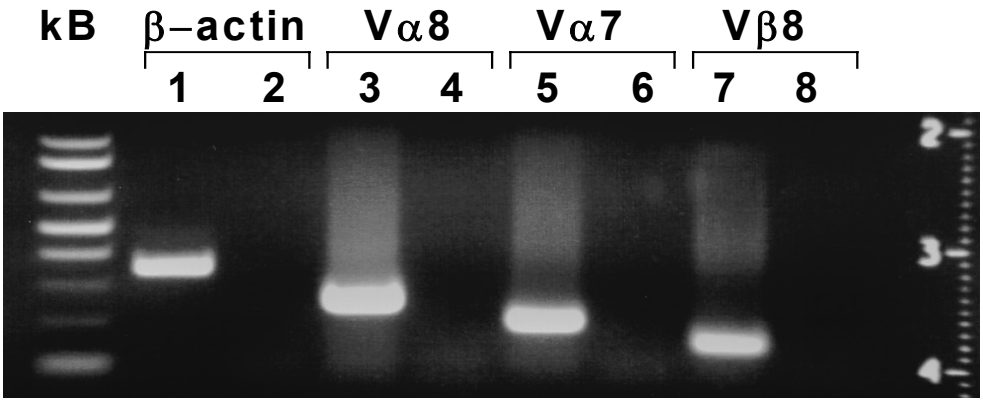

Figure 11. Expression of two TCR α and one β chain by the hsp60 specific $CD8^+$ T cell clone UZ3/4. mRNA expression of TCR chains was confirmed by RT-PCR. cDNA was prepared from the T cell clone UZ 3/4 and amplified with specific screening primers for Vα8.2, Vα7.2 and Vβ8.1 (lane 3, 5, 7, respectively) and β-actin control (lane 1). To exclude DNA contamination of the mRNA preparation, TCR specific PCR was also performed with non reverse transcribed RNA (lane 2, 4, 6, 8).

amplified from cDNA of UZ3/4 adding additional restriction sites at the 5'-end primers, inserted into the TA-cloning vector pCR2.1 and sequenced as described in detail in the methods section. Clones with correct sequences were further subcloned into the plasmids pP142β8AR and pP14αAR to yield full length TCR cDNA containing plasmids p14x–β8 and p14x–α8, respectively. During this procedure the unique V-(D)-J segments of the TCR α8 and TCR β8 were exchanged with those of the p14 TCR α and p14 TCR β contained in the plasmids by making use of the introduced 5' restriction sites and unique internal BanII and EcoRV restriction sites.
To confirm mRNA expression of all three TCR chains in the original clone UZ3/4, RT-PCR analysis using specific screening primers was performed (**Figure 11**). These data clearly show that two successfully in frame rearranged TCR α chain genes and one TCR β chain gene are transcribed in the hsp60 specific T cell clone UZ3/4.

6.2 Surface expression of the TCR α8 chain but not the TCR α7 chain

To study the surface expression of each individual α/β TCR chain combination separately, the full length cDNAs of TCR α7, TCR α8 and TCR β8 were cloned into the retroviral vector pMSCV-IRES-GFP and Phoenix ampho producer cells were transiently transfected with the constructs to produce retroviral vectors. Supernatants were used to efficiently transduce the TCR deficient thymoma cell line 54ζ17. Transduction with the empty vector resulted in over 85% stable transfectants after 48h, and GFP-reporter expression levels remained stable for at least 60 days (data not shown). Transduction of cells with the constructs encoding the TCR α7, TCR α8 or the TCR β8 chain led to approximately 50% GFP positive cells for the TCR α constructs and approximately 40% for the TCR β construct (**Figure 12**). GFP

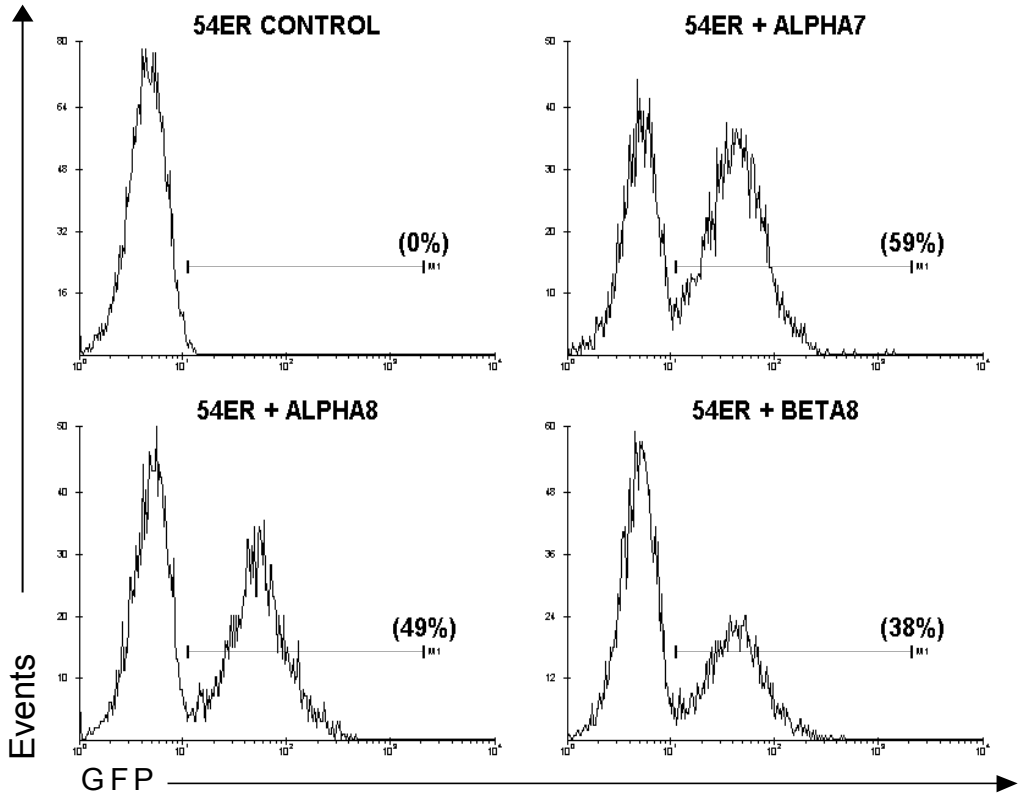

Figure 12. Retroviral transduction of 54ζ17 cells with constructs coding for the TCR chains of the T cell clone UZ3/4. Efficiency of TCR transduction was determined by flow cytometric analysis of the reporter GFP. The numbers above the marker bar indicate the percentage of cells positive for the GFP-reporter.

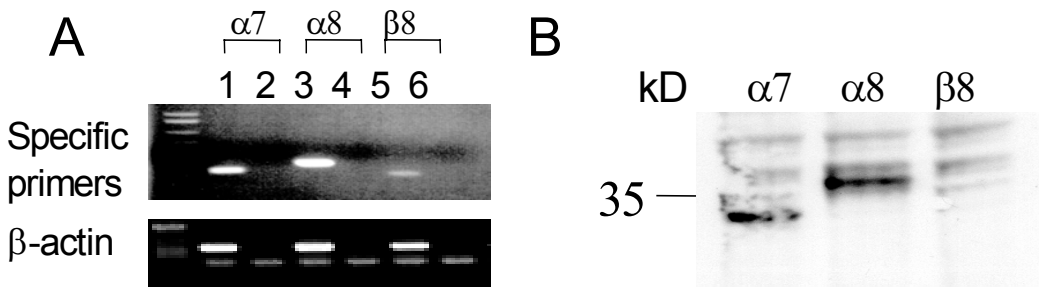

Figure 13. **A)** TCR expression of sorted GFP expressing transfectants by RT-PCR employing specific marker primers for Vα7.2, Vα8.2 and Vβ8.1. PCR was performed with cDNA (lane 1, 3, 5) or non reverse transcribed RNA to control for DNA contamination (lane 2, 4, 6). **B)** Western blot analysis of TCR α chain expression. Lysates of TCR Vα7.2, Vα8.2 and Vβ8.1 transfectants were probed with anti-Cα mAb (H-28 710). Vβ8 transfectants served as negative controls. One representative experiment of three is shown.

positive transfectants were sorted by FACS and expanded. mRNA expression of each single TCR chain was confirmed by RT-PCR with TCR α8, TCR α7 and TCR β8 variable region specific primers (**Figure 13A**). To control for protein expression of both α chains, Western blot analysis was performed using a mAb specific for the constant portion of the TCR α chain (**Figure 13B**). The calculated masses of TCR α7 and TCR α8 are similar, 30.7 kD vs. 30.9 kD for the whole protein, and 28.6 kD vs. 28.5 kD after cleavage of the signal peptide, respectively. Interestingly, the TCR α8 protein migrated markedly slower in the SDS gel compared to the TCR α7 protein. This may reflect differential posttranslational modification, since the Vα7 chain lacks extracellular N-glycosylation sequences that are present in the Vα8 chain (Ronin et al., 1978).

To determine whether both α chains could form a functional TCR by pairing with TCR β8, we produced double transfectants for each TCR αβ combination and analyzed cell surface expression of both potential heterodimers on these cells. GFP-sorted TCR β8 transfectants did not show any TCR surface expression, indicating that only complete αβ TCR heterodimers can be expressed at the cell surface in this system. Therefore, surface expression of the TCR α chains could be indirectly measured using specific mAb directed against the TCR β8 chain.

TCR β8 transfectants were transduced with either the TCR α7 or the TCR α8 chain. Upon transduction of TCR α8, approximately 50% of the cells revealed surface expression of TCR β8 as evidenced by FACS analysis (**Figure 14A**). Since the transduction efficiency of the TCR α vectors for the parental cell line 54ζ17 was in the same range (**Figure 12**), these results suggest efficient surface expression of the α8 and β8 TCR chain combination. Unexpectedly, transduction with the TCR α7 construct did not result in detectable TCR surface expression in TCR β8 transfected cells (**Figure 14A**), although the transduction efficiency of the TCR α7 and TCR α8 constructs was comparable, as shown for the parental cell line 54ζ17 (**Figure 12**). Given that both α chains were comparably expressed as shown by western blot (**Figure 13B**), these results strongly suggest inefficient surface expression of the TCR α7 and TCR β8 chain combination. This finding was independent of the order of transduction, similar results were obtained when TCR α7 or TCR α8 chain transfectants were transduced with the TCR β8 construct (**Figure 14B**). Additionally, TCR surface expression in TCR α8 and TCR β8 but not in TCR α7 and TCR β8 double transfectants was confirmed with mAb specific for the constant part of TCR β chains and with mAb specific for CD3 complex proteins (data not shown).

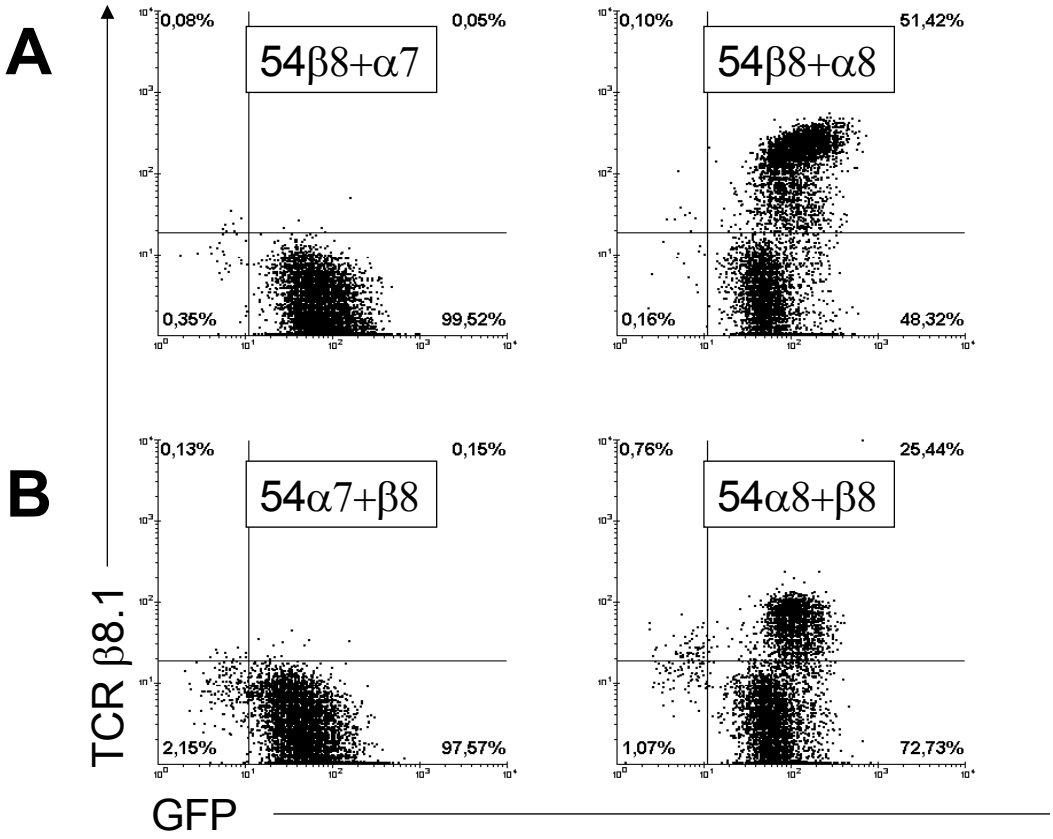

Figure 14. TCR surface expression of TCR α8/β8 but not TCR α7/β8 transfectants by flow cytometry. **A)** TCR Vβ8.1 were transduced with pMSCV-IRES-GFP vectors containing the cDNA for TCR Vα7.2 or Vα8.2. **B)** TCR Vα7.2 or Vα8.2 transfected 54ζ17 cells (54α7 or 54α8) were transduced with pMSCV-IRES-GFP vector containing the cDNA for TCR Vβ8.1. After 48h, TCR surface expression was determined by flow cytometry. The numbers in the upper right quadrants indicate the percentage of GFP-marker and surface TCR double positive cells. One of two independent experiments is shown.

6.3 Promiscuous peptide recognition of mycobacterial and murine peptides by the α8/β8 TCR combination

Previous analyses have shown that the autoreactive CD8+ T cell clone UZ3/4 recognizes hsp60 derived peptides of both mycobacterial and murine origin (Zugel et al., 1995). To functionally examine whether this cross-reactivity is mediated by the α8/β8 TCR combination, CTL assays were performed in the presence or absence of mAb specific for either TCR Vβ8 or TCR Vα8. Addition of both of these mAb efficiently blocked the cytolytic activity of the CD8+ T cell clone UZ3/4 in response to both peptides (**Figure 15**). Addition of isotype control mAb had no effect (data not shown). To confirm these results, we determined whether transfectants displaying only the α8/β8 TCR responded to the same peptides as the hsp60 specific CD8+ T cell clone. Therefore, α8/β8 TCR double transfectants were cocultured with spleen cells from C57BL/6 mice in the presence or absence of hsp60 and control peptides. A specific response to both the mycobacterial and the murine hsp60 peptides was detected by upregulation of the very early activation marker CD69 (**Figure 16**). These results confirm that the α8/β8 TCR combination is capable of promiscuous peptide recognition of mycobacterial as well as murine peptides presented on H2-D^b.

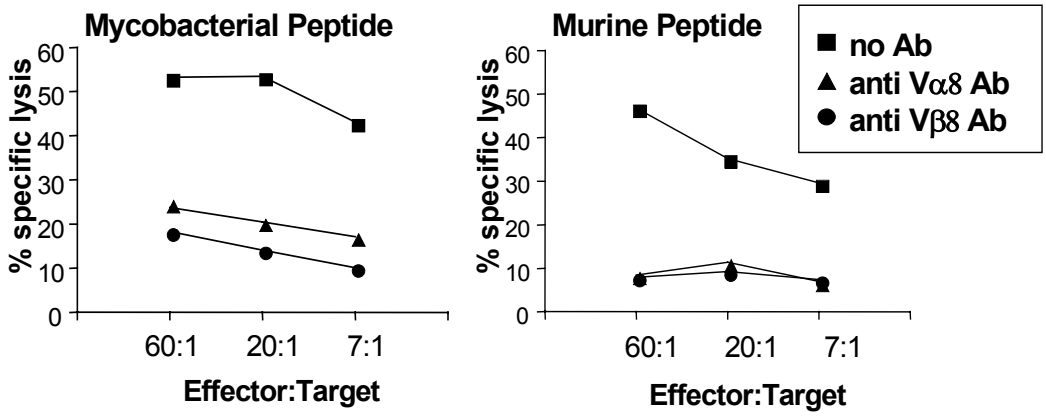

Figure 15. ^{51}Cr release assay using EL 4 cells pulsed with the mycobacterial or murine hsp60 peptide as targets. Cytolytic activity of the hsp60 specific T cell clone against target cells is determined at the given effector : target ratios in the presence of mAb specific for Vα8 or Vβ8. One representative experiment of three is shown.

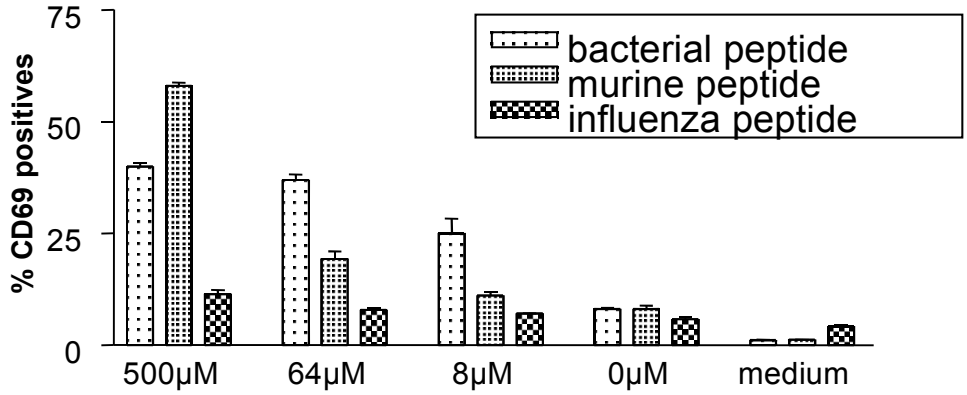

Figure 16. Crossrecognition of bacterial and murine hsp60 peptides is mediated by the TCR Vβ8.1 and Vα8.2 chain combination. TCR α8/β8 transduced 54ζ17 cells were stimulated with the indicated amounts of the mycobacterial (SALQNAASIA) and murine (KDIGNIISDA) hsp60 peptides. After 20h, CD69 upregulation was assessed by FACS analysis. One representative experiment of three is shown.

6.4 Generation of TCR α8 and TCR β8 transgenic mice

Having determined the functional TCR combination of the hsp60 specific T cell clone UZ3/4, our goal was the generation of transgenic mice with germline integration of the corresponding rearranged TCR genes. Therefore, full length cDNA of the TCR α8 and TCR β8 chains was cloned into the TCR expression vector pHSE3'. To test the functionality of the constructs, TCR expression was tested in the TCR deficient thymoma cell line 58α⁻β⁻. The pUC18 backbone was removed from the constructs and the linearized vectors together with a linearized plasmid containing a Zeocin resistance gene were used to electroporate 58α⁻β⁻ cells. Transfected cells were cultured in the presence of zeocin at a concentration of 300µg/ml. TCR α8 and TCR β8 stable transfectants showed cell surface expression of the TCR as tested with TCR Vα8 and TCR Vβ8 specific mAbs (**Figure 17**). After confirming TCR expression in cell lines that integrated the constructs into their genome, the linearized vectors were used to generate TCR transgenic mice. Therefore, they were microinjected into the male pronucleus of eggs from CBA x C57BL/6 F1 female mice fertilized by C57BL/6 males. The constructs for both TCR chains were co-injected, a procedure that usually results in co-integration of both constructs at the same site of a chromosome leading to co-transmission to the next generation. Using this method, only one double positive founder was obtained and unfortunately, this mouse died before it could be further analyzed and no offspring were produced. To circumvent possible adverse effects of the transgenic expression of a potentially autoreactive α8 β8 TCR during the development of the TCR transgenic mice, the strategy was changed and the

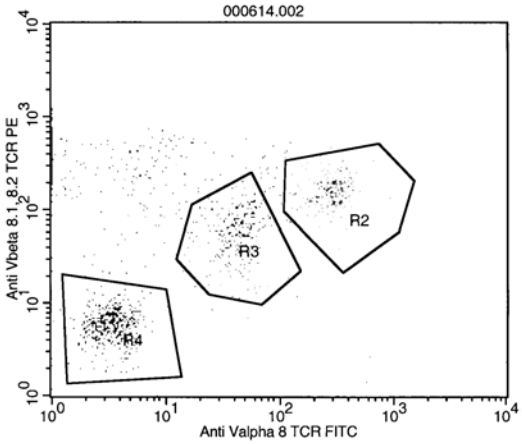

Figure 17. Triple transfection of BW derived TCR deficient cell lines with the pHSE-expression constructs and a plasmid containing Zeocin® resistance resulted in stable cell lines expressing the TCRα8/β8 at different levels. Zeocin® selected cells were stained wit mAb specific for TCR α8 and β8 R2: population with high TCR expression, R3: low TCR expression, R4: no TCR expression.

constructs were injected separately. This procedure resulted in 13 TCR α8 and 3 TCR β8 transgenic founder mice that are listed in **Table 4**. Offspring (potential founders) were screened for the integration of the transgenic TCR α8 and β8 chain constructs by PCR of tail biopsy derived DNA (**Figure 18**). Further, the expression of the transgenic TCR chains was analyzed by flow cytometry of peripheral blood cells (**Figure 19 and Figure 20**).

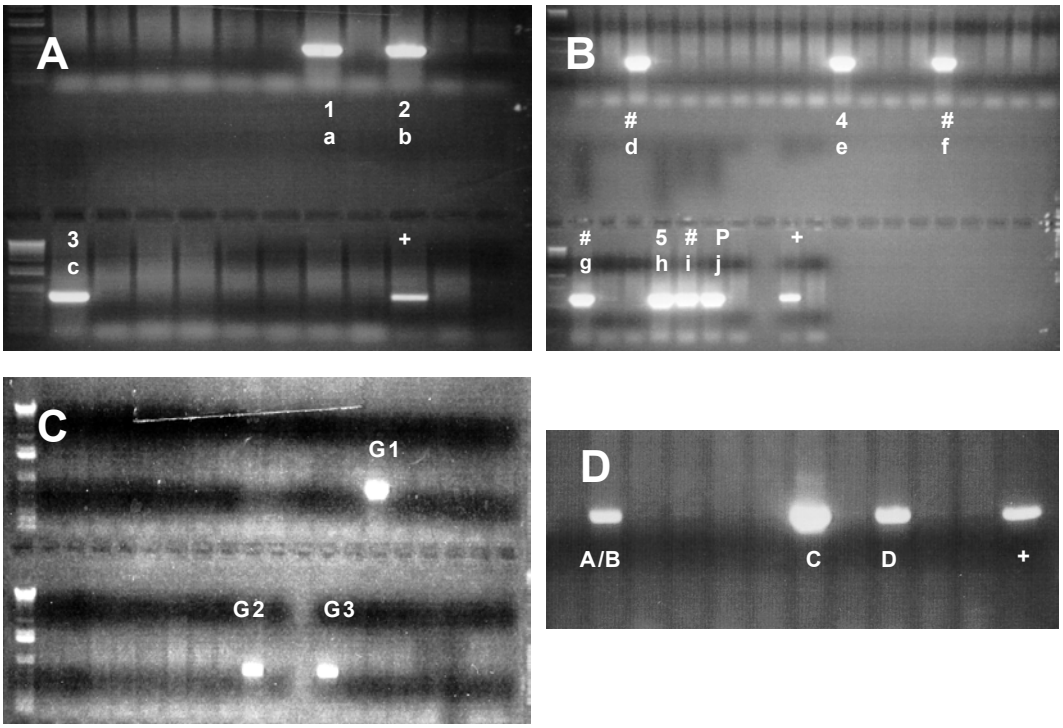

Figure 18. PCR screening of potential founder mice. DNA derived from tail biopsies was analyzed using construct specific primer pairs for TCR α8 and TCR β8. (**A-C**) The letters a-j and G1-G3 indicate individual TCR α8 founders. Animals marked 1-5 were initially used to establish individual transgenic lines, the founder j (labeled P) was directly crossed to TCR β8 -C. (**D**) The letters A-D indicate individual TCR β8 founders, all these were initially used to establish individual transgenic lines.

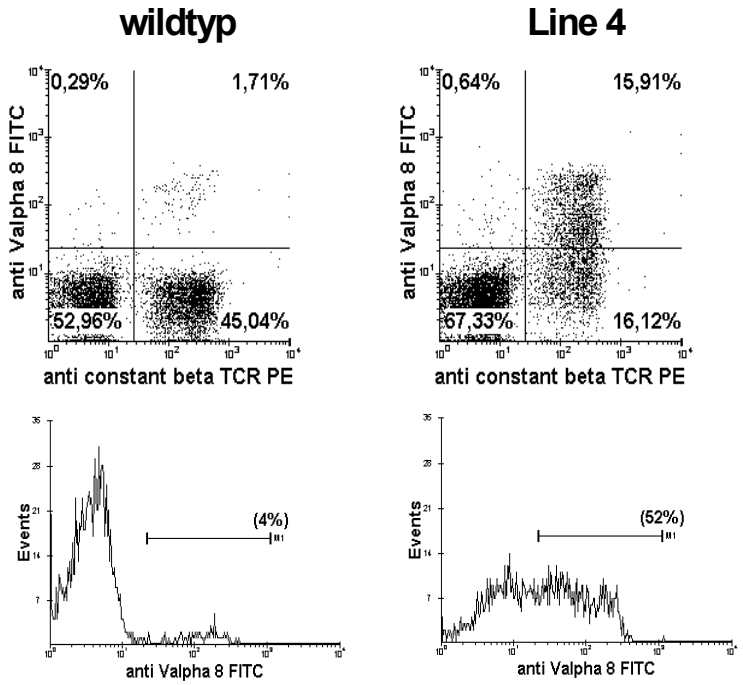

Figure 19. Principle of screening for potential TCR α8 founders by flow cytometric analysis. PBL from wildtyp and transgenic mice were stained with mAb specific for the constant region of the TCR β chain and mAb specific for the TCR Vα8 segment. Upper panel: Dot blots showing profiles of TCR β and TCR Vα8 expression. The percentage of cell subsets is shown in each dot plot quadrant. Lower panel: TCR β positive cells were gated, marker in histograms showing the percentage of TCR Vα8 positive among TCR αβ positive cells.

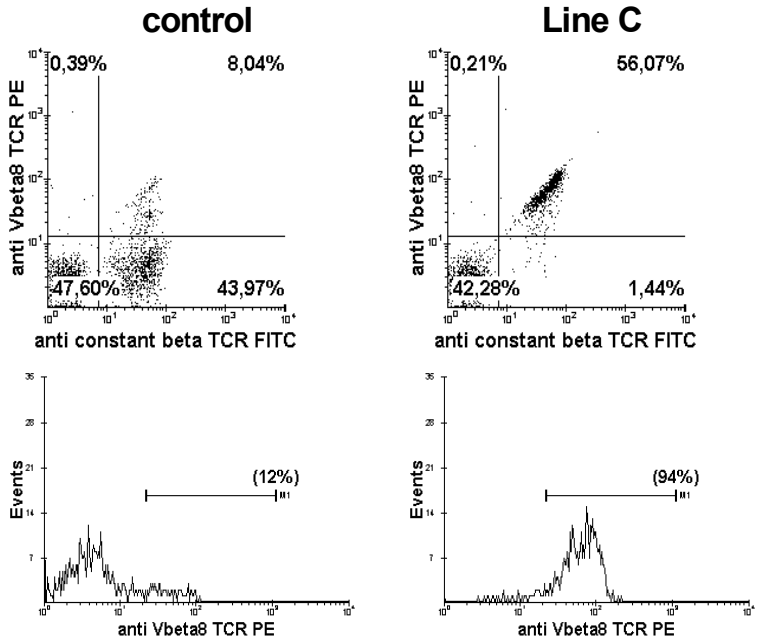

Figure 20. Principle of screening for potential TCR β8 founders by flow cytometric analysis. PBL from wildtyp and transgenic mice were stained with mAb specific for the constant region of the TCR β chain and mAb specific for the TCR Vβ8 segment. Upper panel: Dot blots showing profiles of TCR β and TCR Vβ8 expression. The percentage of cell subsets is shown in each dot plot quadrant. Lower panel: TCR β positive cells were gated, marker in histograms showing the percentage of TCR Vβ8 positive among TCR αβ positive cells.

Expression levels of the transgenic TCR chains in peripheral blood lymphocytes (PBL) varied greatly among individual founders. **Table 4** represents a list of the TCR α8 and TCR β8 transgenic mice, including expression levels of the transgene, and their current breeding status. In two lines, α8-3 and β8-D, expression of the transgene was significantly higher in the F-1 generation compared to the founders (F-0). This elevated transgene expression was transmitted to the F-2 generation only in the α8-3 but not in the β8-D line. To obtain mouse lines with stable transgenic expression, offspring from various founder mice with different expression levels were bred as individual lines by back-crossing them 3-4 times to inbred C57BL/6 mice. The lines α8-3, α8-4 and β8-C are stable lines and are maintained in the specific pathogen-free breeding area of the BgVV. The TCR α8 founder # j, named line P, was crossed with β8-C mice to study α8 and β8 double transgenic mice while waiting for the breeding of stable lines.

Founder	Transgene	Line	Expression of transgenic TCR chain in %	Status
1	α8, β8	-	n.d.	No offspring
a	α8	1	16	retired
b	α8	2	8	retired
c	**α8**	**3**	**6 F-0 / 26 F-1**	**breeding**
d	α8	-	2	not bred
e	**α8**	**4**	**45**	**breeding**
f	α8	-	1	not bred
g	α8	-	7	not bred
h	α8	5	45	retired
i	α8	-	-	not bred
j	α8	P	18	Preliminary crossing to line β8-C
G1	α8	-	7	not bred
G2	α8	-	2	not bred
G3	α8	G	60	breeding
A/B	β8	-	-	not bred
C	**β8**	**C**	**>90**	**breeding**
D	β8	D	0 / 20 in F-1	retired

Table 4. Overview of the generated TCR α8 and β8 transgenic mice. Values of TCR α8 expression are calculated as percentage of TCR Vα8 positive PBC minus 4% wildtype TCR Vα8 positive PBL. The TCR α8 expressing lines 3 and 4, and the TCR β8 expressing line C are stable lines breeding in the specific pathogen-free breeding area of the BgVV. The α8-P line was crossed to line β8-C to obtain preliminary data on α8 and β8 double transgenic mice.

6.5 Peripheral TCR α8 and β8 double transgenic mice are specific for the peptide SALQNAASIA from mycobacterial hsp60

Offspring from crosses of mouse lines β8-C and α8-P were analyzed for expression of the transgenic TCR chains and the T cell coreceptor CD8. The genotype was determined by PCR screening. In the periphery of β8-C and α8-P double positive mice elevated frequencies of T cells expressing both Vα8 and Vβ8 TCR chains were found (**Figure 21**). 3-4% of the PBL were Vα8 and Vβ8 TCR double positive compared to 0.2% in non-transgenic littermates. This number corresponds with the frequency of 3-4% TCR Vα8 positive PBC in α8-P single transgenic mice. Given that greater than 90% of the T cells in β8-C mice express the transgenic β8 TCR, these findings suggest that T cells expressing both the TCR α8 and TCR β8 transgene are positively selected in the thymus.

The large majority (greater than 75%) of these Vα8 and Vβ8 TCR double positive T cells expressed the CD8 T cell coreceptor and represent 20-25% of the peripheral

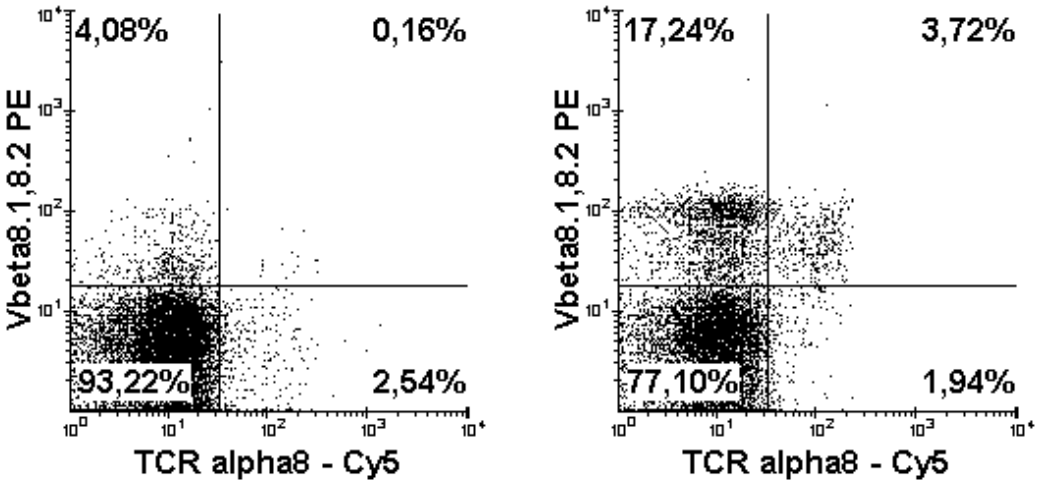

Figure 21. Elevated frequencies of Vα8 and Vβ8 TCR double positive T cells appear in the periphery of β8-C and α8-P double transgenic mice. PBL of control (left) and transgenic (right) mice were stained with Cy5-conjugated anti-TCR Vα8 mAb, FITC-conjugated anti-CD8 mAb, and PE- conjugated anti-TCR Vβ8 mAb. Dot blots showing profiles of TCR Vα8 and TCR Vβ8 expression. The percentage of cell subsets is shown in each dot plot quadrant.

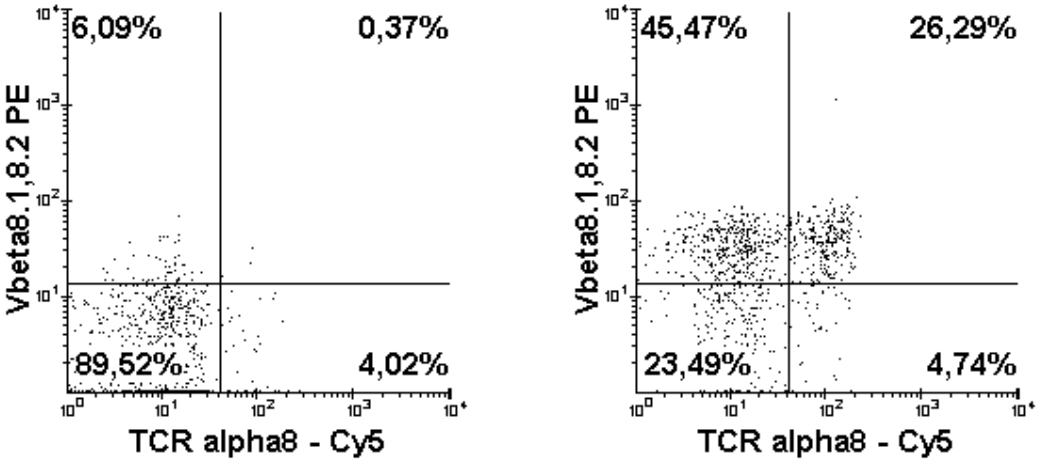

Figure 22. Same as figure 21, gated on CD8 positive cells.

CD8+ T cells (**Figure 22**). In contrast, in PBL of non-transgenic littermates only 10-15% of Vα8 and Vβ8 TCR double positive T cells express the CD8 T cell coreceptor and less than 0.5% of the peripheral CD8+ T cells were α8 and Vβ8 TCR double positive. As expected, these results reveal that the phenotype of TCR α8 and TCR β8 double transgenic thymocytes is identical to the original clone UZ3/4 from which the TCR chains were cloned. The cells are positively selected during thymic maturation as MHC class I restricted, CD8 coreceptor dependent T cells.

Next, we tested whether the TCR α8 and TCR β8 double transgenic thymocytes were specific for the mycobacterial hsp60 derived peptide SALQNAASIA ($hsp60_{499-508}$) that was recognized by the original CTL clone UZ3/4. Therefore, we generated H2-D^b MHC class I-peptide tetramers containing the $hsp60_{499-508}$ peptide. PBL were stained with the tetramers and analyzed by flow cytometry (**Figure 23**). Although the signal of tetramer positive cells was only separated from the background, we found a distinct T cell population that bound the PE-labeled $hsp60_{499-508}$ MHC class I tetramers in the TCR transgenic but not in non-transgenic littermates. These data clearly show that the transgenic TCR in β8-C and α8-P double positive mice specifically recognizes the same mycobacterial hsp60 peptide as the original T cell clone UZ3/4.

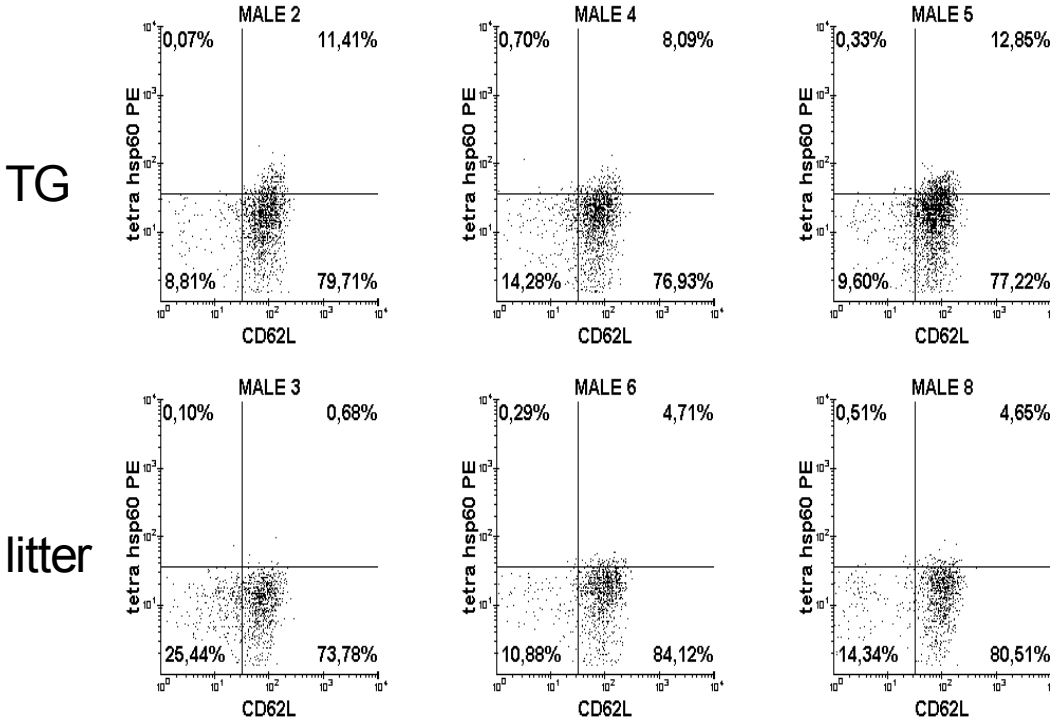

Figure 23. Specific staining of T cells from β8-C and α8-P double positive mice with $hsp60_{499-508}$ MHC class I tetramers. PBL were stained with Cy5-conjugated anti-CD8 mAb, FITC-conjugated anti-CD62L mAb, and PE-labeled $hsp60_{499-508}$ MHC class I tetramers and analyzed by 4-color flow cytometry after addition of propidium iodide. Upper panel: Histograms showing live-gated, propidium iodide-negative CD8+ IEL from 3 male β8-C and α8-P double positive mice, and lower panel: from 3 non-transgenic littermates. The percentage of T cell subsets is shown in each dot plot quadrant.

6.6 Induction of CD8+ T cells specific for SALQNAASIA mycobacterial hsp60 peptide during mycobacterial infection

In normal C57BL/6 mice, hsp60 specific T cells participate in BCG induced immune responses to mycobacterial infection. It has recently been shown that CD8+ cells specific for the mycobacterial hsp60 peptide 499-508 were activated *in vivo* by BCG vaccination, (Zugel and Kaufmann, 1997). These T cells, however, were restimulated *in vitro* with APC presenting the mycobacterial peptide SALQNAASIA for several weeks in the presence of activating cytokines. Hence it could be argued that this model does not adequately reflect the proportion of hsp60 specific CD8+ T cells in an *in vivo* situation.

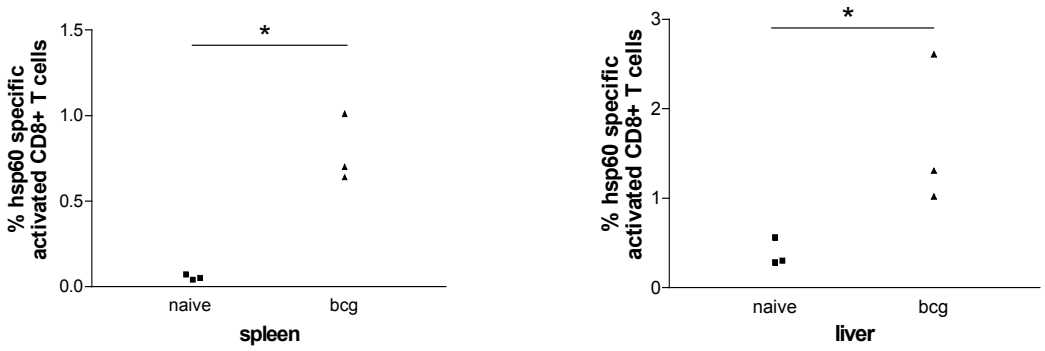

Figure 24. Mice were infected with 5 x 10^6 BCG, after 24 days, spleen and liver cells were stained with Cy5-conjugated anti-CD8 mAb, FITC-conjugated anti-CD62L mAb, and PE-labeled hsp60$_{499-508}$ MHC class I tetramers and analyzed by 4-color flow cytometry after the addition of propidium iodide. Individual data points of 3 mice per group are shown. Data were analyzed by the Mann-Whitney unpaired T test, P values < 0.05 were considered significant.

To analyze the number of CD8+ T cells specific for the mycobacterial hsp60 peptide SALQNAASIA in an immune response against mycobacterial infection, *ex vivo* frequencies of CD8+ T cells specific for the hsp60$_{499-508}$ tetramers were determined in the spleen, liver, and IEL. Previous studies have described highest frequencies of CD8+ T cell responses in an interval of time between 20-30 days after BCG immunization (Grode et al., 2002). Therefore, the time point for tetramer analysis of activated, peptide-specific cells was chosen 24 days after immunization (**Figure 24**). In addition, cells were isolated 21 days after immunization and subsequently

restimulated *in vitro* for 4 days with the $hsp60_{499-508}$ peptide (**Figure 25**). We found significantly higher frequencies of $hsp60_{499-508}$ peptide specific CD8+ T cells in the analyzed organs of BCG infected mice compared to naive mice.

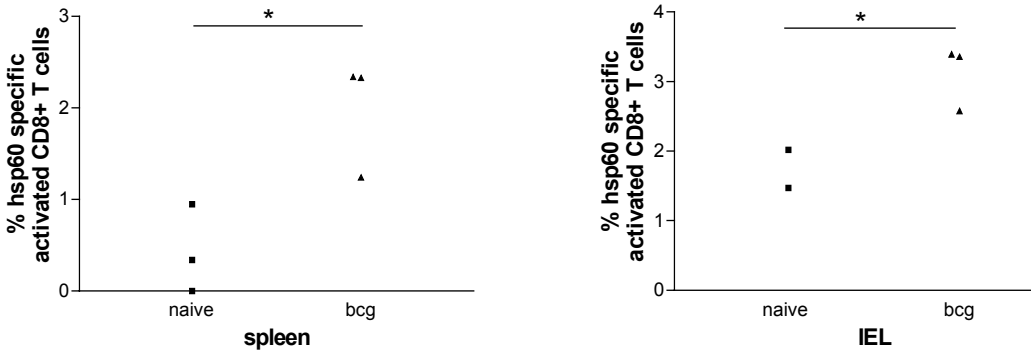

Figure 25. Mice were infected with 5 x 10^6 BCG, after 21 days, spleen and cells and IEL were cultured with APC and 2µM $hsp60_{499-508}$ peptide. After 4 days cells were stained with Cy5-conjugated anti-CD8 mAb, FITC-conjugated anti-CD62L mAb, and PE-labeled $hsp60_{499-508}$ MHC class I tetramers and analyzed by 4-color flow cytometry after the addition of propidium iodide. Individual data points of 3 mice per group are shown. Data were analyzed by the Man-Whitney unpaired T test, P values < 0.05 were considered significant.

In an additional experiment, it was tested whether the activation of mycobacterial hsp60 specific CD8+ T cells could be induced by peptide immunization. Mice were immunized subcutaneously (s.c.) weekly a total of 1-3 times with 40µg of $hsp60_{499-508}$ peptide in incomplete Freud's adjuvant (IFA). Elevated frequencies of $hsp60_{499-508}$ peptide specific CD8+ T cells were observed in spleen or the draining sarcoid lymph node (SLN) (**Figure 26**). However, no significant differences in the frequencies of peptide specific CD8+ cells could be observed between the test groups indicating that the number of times the peptide was administered had no effect .

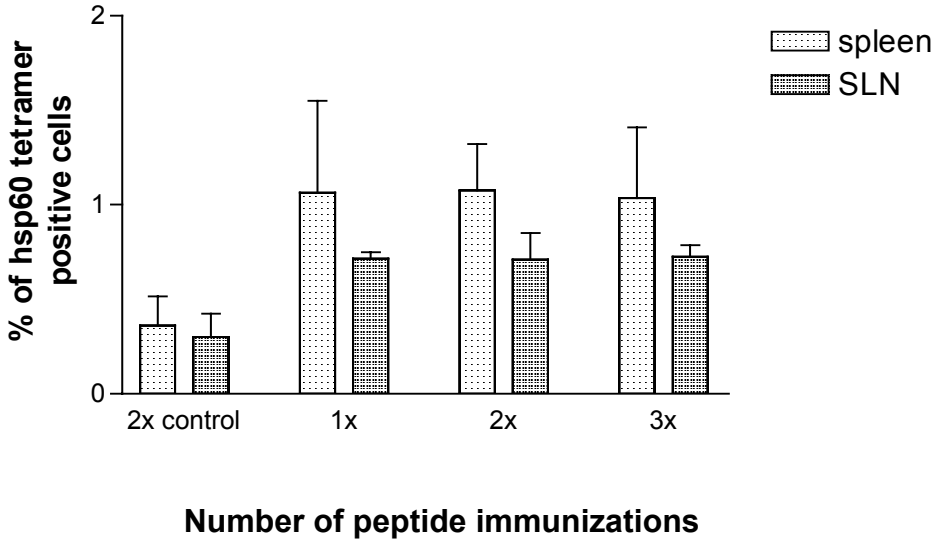

Figure 26. Mice were immunized 1-, 2-, or 3- times with 40µg $hsp60_{499-508}$ peptide s.c. in IFA, 3 days after the last immunization, spleen cells and SLN cells were stained with Cy5-conjugated anti-CD8 mAb, FITC-conjugated anti-CD62L mAb, and PE-labeled $hsp60_{499-508}$ MHC class I tetramers and analyzed by 4-color flow cytometry after the addition of propidium iodide. Data are given as mean ± SD values of $tetramer^{+}$ $CD62L^{low}$ cells of live CD8+ T cells of 2 mice per group.

6.7 Generation of TCR α7 transgenic mice

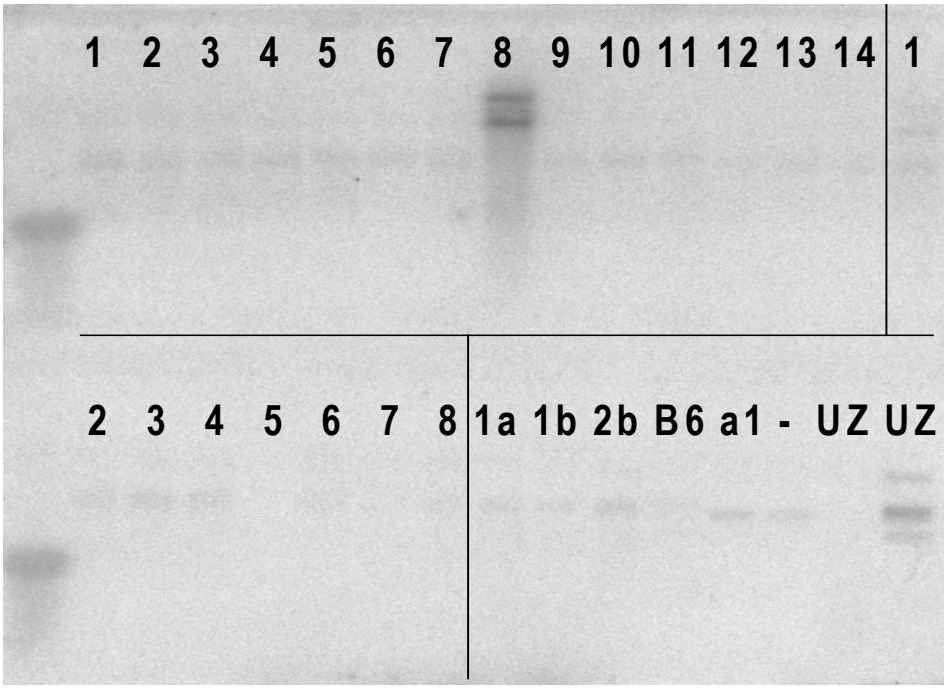

Figure 27. Screening of potential TCR α7 transgenic founders. Tail biopsy DNA was analyzed by Southern blotting using a 32P-labeled TCR Va7.2 specific probe.

In section 6.2 it was shown that in contrast to the TCR α8 chain, the TCR α7 chain was unable to form a functional TCR with the corresponding TCR β8 chain. To evaluate whether TCR α7 can pair productively with any other TCR β chain, we generated TCR α7 transgenic mice and crossed them with TCR $\alpha^{-/-}$ mice (α -/- mice). A genomic TCR expression construct (containing an original TCR promoter and intron and exon structures) was used and the mice were generated on a pure C57BL/6 background to keep the conditions as close to the physiological situation as possible. The recombined VJ segments of the TCR α7 chain were cloned into the pSHVα T cell receptor expression cassette and the linearized construct was injected into the pronucleus of fertilized eggs from C57BL/6 mice. Potential founder mice were screened by PCR and Southern blotting. One positive founder was obtained and bred as an individual mouse line (**Figure 27**). TCR α7 transgene positive mice had no obvious phenotype, yet stable expression of the transgenic TCR α7 was transmitted over 3 generations as determined by diagnostic RT-PCR based on our

construct (**Figure 28**). Transgenic TCR α7 mice were crossed to α -/- mice. α -/- mice expressing the transgenic TCR α7 chain are subsequently termed α 7.2 mice, control littermates that have at least one intact TCR α chain locus are termed α +/- mice.

In α 7.2 mice TCR α7 expression was found in the thymus as well as in peripheral lymphocytes as determined by RT-PCR (**Figure 29**). The large majority of their thymocytes was arrested in the double positive stage (**Figure 30**). Nevertheless, low but significantly increased frequencies of single positive cells were detected in thymi derived from α 7.2 mice compared to thymi from α -/- mice (**Figure 30**). However, the expression of the TCR α7 chain in α -/- mice did not restore conventional CD4+ and CD8+ T cells with respect to TCR αβ expression levels comparable to normal mice (**Figure 31A**). These findings suggest that TCR α7 cannot form a normal TCR αβ with any endogenous TCR β chain.

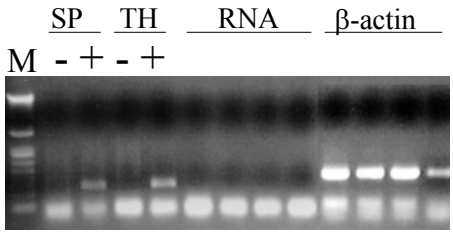

Figure 28. Transgenic expression of TCR α7 in C57BL/6 mice. RT-PCR shows TCR α 7.2 chain expression in spleen (SP) and thymus (TH) derived lymphocytes of transgenic TCR α7 mice (+) compared to non-transgenic littermates. Non reverse-transcribed RNA was used as negative, β-actin as positive control.

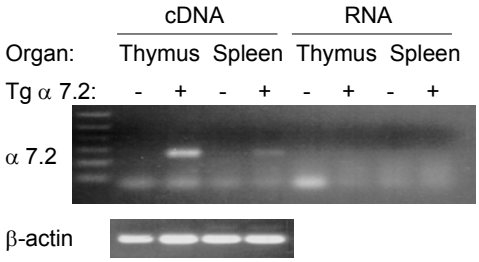

Figure 29. Transgenic expression of TCR α 7 in TCR $\alpha^{-/-}$ mice. RT-PCR shows TCR α 7.2 chain expression in thymus and spleen derived lymphocytes of α 7.2 mice (+) compared to non-transgenic littermates. Non reverse-transcribed RNA was used as negative, β-actin as positive control.

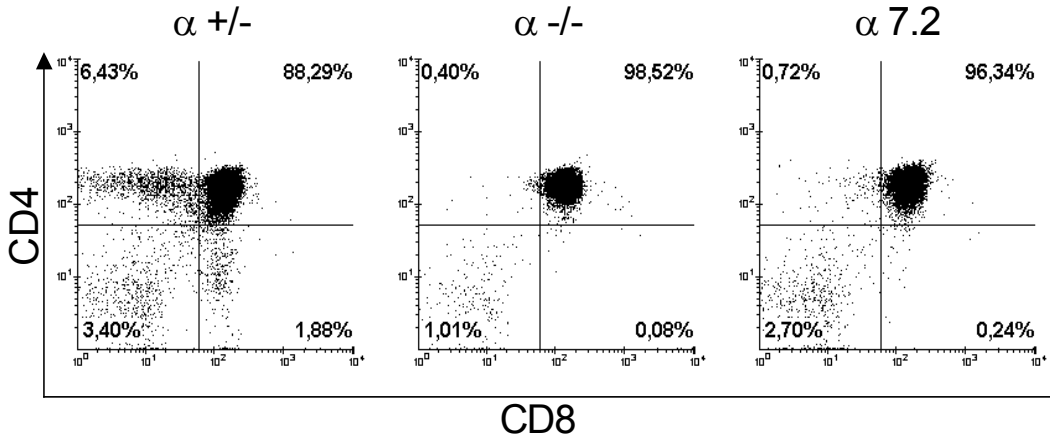

Figure 30. Impaired T cell maturation in α 7.2 mice. T cell differentiation was analyzed by staining thymocytes from 6 weeks old mice for CD4 and CD8. Data are representative of three independent experiments.

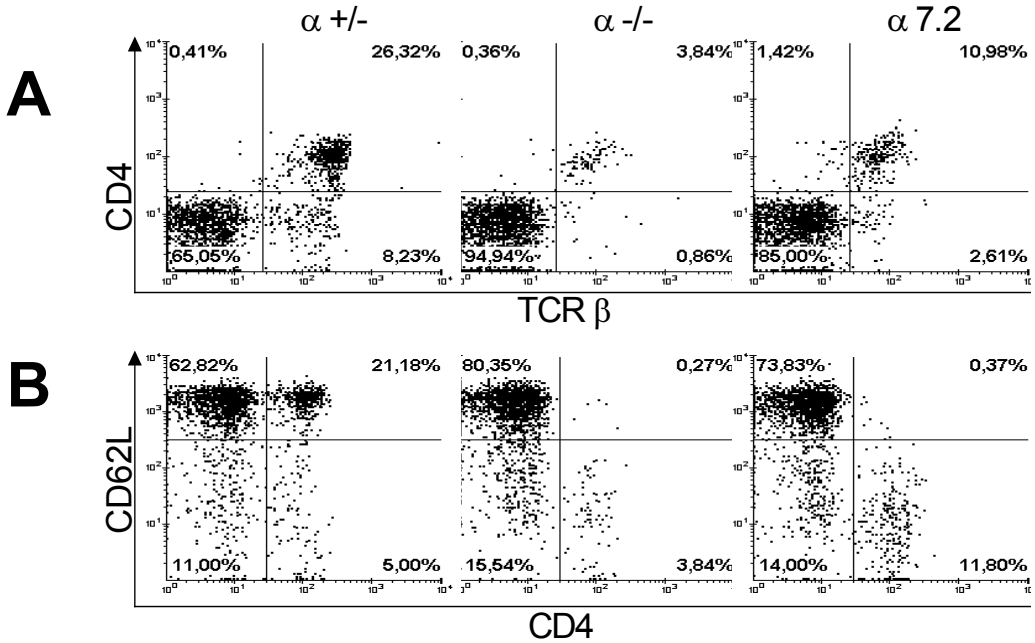

Figure 31. Increased frequencies of CD4+ TCR β^{low} T cells in α 7.2 mice. Peripheral blood cells (PBC) from α 7.2, α -/- and α +/- littermate mice at 4-6 weeks of age were stained for CD4, CD8, CD62L and TCR β chain surface expression. (**A**) Dot plots show TCR β and CD4 expression profiles of PBC of the indicated mice. The percentage of T cell subsets is shown in each dot plot quadrant. (**B**) Dot plots showing CD4 and CD62L expression profiles of PBC of the same mice. FACS profiles are representative of at least five independent experiments.

6.8 Augmented levels of CD4+ TCR $\alpha^{-}\beta^{+}$ T cells in α 7.2 mice

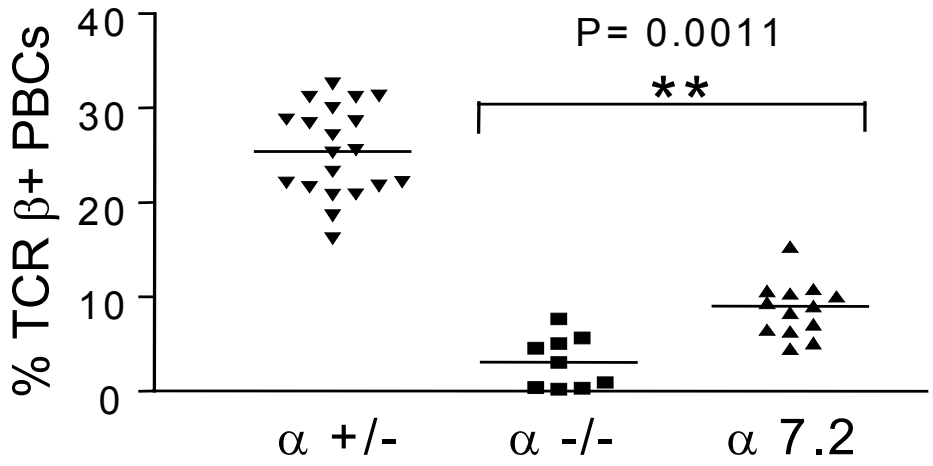

Figure 32. Comparison of the frequencies of TCR β positive cells in PBC of the indicated mice. The symbols represent the percentage of TCR β positive cells in PBC of each individual mouse for the α +/-, α -/-, and α 7.2 mice test groups.

Next, the TCR expression profile of blood derived lymphocytes was compared between α 7.2 mice, α -/- mice and heterozygous control mice (α +/-). The percentage of lymphocytes expressing surface TCR β was significantly higher in α 7.2 mice compared to α -/- mice but never reached levels of α +/- control mice (**Figure 32**). Frequencies of peripheral blood CD4+ TCR$\alpha^{-}\beta^{+}$ T cells in α 7.2 and α -/- mice were analyzed by the Mann-Whitney unpaired t-test. *P* values < 0.05 were considered significant. The TCR β positive cells in α 7.2 mice were phenotypically indistinguishable from those found in α -/- mice (Mombaerts et al., 1992). In both strains, the expression level of TCR β was low compared to α +/- controls and most T cells expressed the CD4 coreceptor (**Figure 31A**). Interestingly, peripheral blood CD4 + T cells from both α 7.2 and α -/- mice exhibited an activated blast phenotype with more than 90% expressing low levels of CD62L (L-selectin) (**Figure 31B**). In contrast, 80% of peripheral CD4+ T cells in α +/- mice were CD62L high (**Figure 31B**). These results suggest that the population of peripheral CD4+ TCR β^{low} T cells found in α 7.2 mice differs from wild-type CD4+ αβ T cells and represents an equivalent to the CD4+ TCR $\alpha^{-}\beta^{+}$ T cells found in the periphery of α -/- mice.

6.9 CD4+ TCR $\alpha^{-}\beta^{+}$ T cells show an activated phenotype

We next examined the activation status of peripheral CD4+ T cells derived from secondary lymphatic organs, i.e. spleen and mesenteric lymph nodes (MLN) by flow cytometry. In contrast to α +/- controls, the large majority (80-90%) of the CD4+ T cells from α 7.2 and α -/- mice was CD62L low and CD44 high indicating an activated phenotype (**Figure 33A**). Also, the CD4+ T cells from α 7.2 and α -/- mice showed increased upregulation of the very early activation marker CD69 (**Figure 33B**). However, CD69 upregulation was more pronounced in the MLN, as compared to the spleen lymphocytes. Thus, the CD4+ T cells from both α 7.2 and α -/- mice differ from normal CD4+ T cells not only with respect to TCR expression levels, but also in their activation status. Hence, CD4+ TCR $\alpha^{-}\beta^{+}$ T cells are chronically activated.

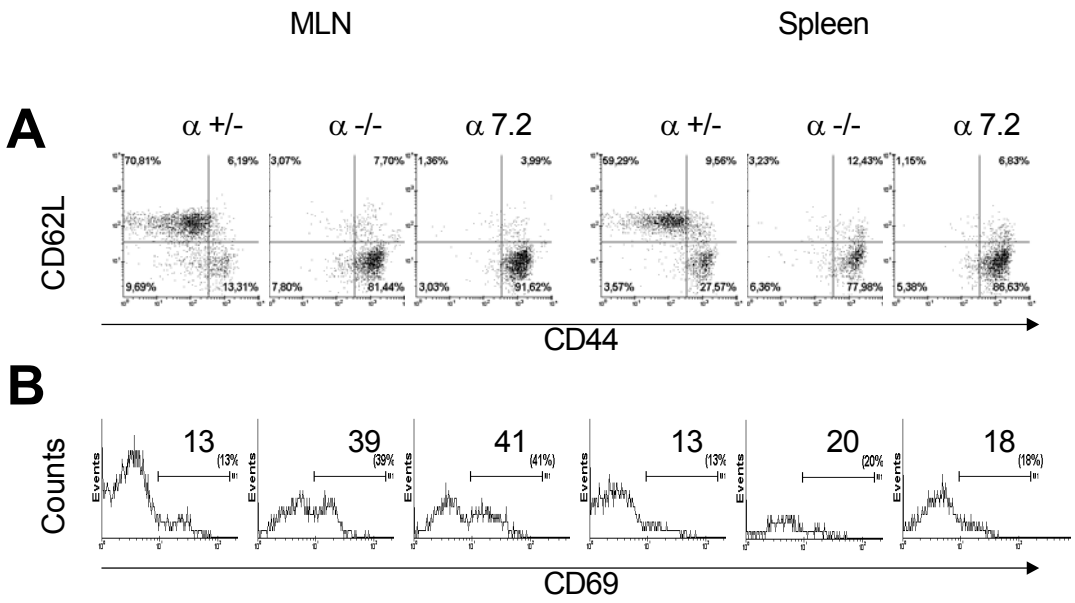

Figure 33. Peripheral CD4+ TCR $\alpha^{-}\beta^{+}$ T cells are chronically activated. Cells were prepared from mesenteric lymph nodes (MLN) and spleens of 6-week-old α 7.2, α -/- and α +/- littermates and stained for expression of the cell surface activation markers CD44, CD62L and CD69 plus CD4. (**A**) Cells were gated on CD4, dot plots show CD44 and CD62L activation marker profiles. The percentage of T cell subsets is shown in each dot plot quadrant. (**B**) Cells were gated on CD4 expression, histograms showing expression of CD69 activation marker. Similar results were obtained from three independent experiments.

6.10 Accelerated course of IBD in α 7.2 mice

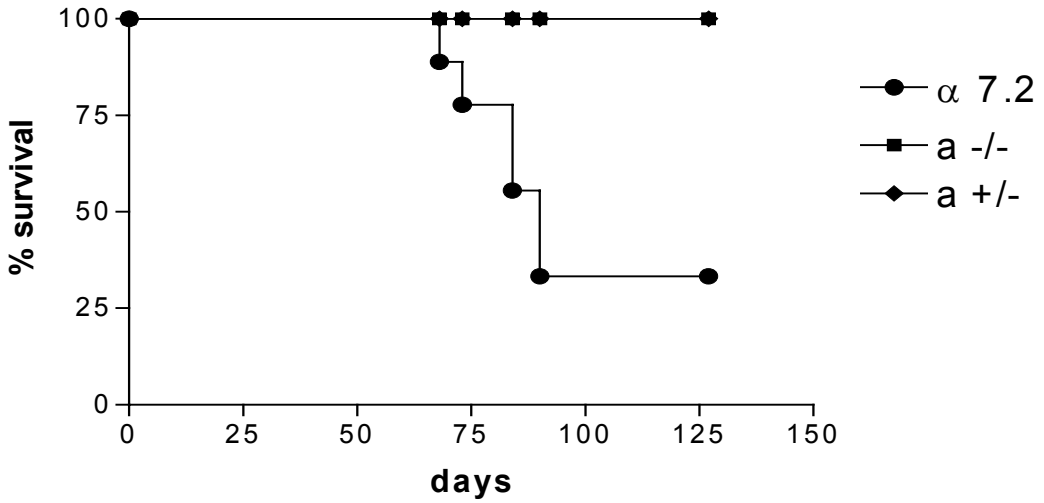

Figure 34. Accelerated course of IBD in α 7.2 mice. α 7.2, α -/- and α +/- littermate mice from heterozygous breedings were monitored for 4 months. At an age of 8 weeks, α 7.2 mice began to develop severe IBD characterized by chronic diarrhea and progressive wasting syndrome. α -/- and α +/- littermates remained disease free during the period of observation. At least 8 mice per group were observed for each genotype. Data are from two independent experiments that gave consistent results.

Previously, it has been suggested that CD4+ TCR$\alpha^{-}\beta^{+}$ T cells are responsible for induction of a Th2 biased colitis in α -/- mice (Mizoguchi et al., 1997b; Takahashi et al., 1997). To analyze the impact of the augmented CD4+ TCR $\alpha^{-}\beta^{+}$ T cell population on the occurrence and severity of the disease, littermate α +/-, α -/- and α 7.2 mice were observed over a period of 4 months. While α +/- and α -/- animals remained disease free, fatal IBD developed in α 7.2 mice (**Figure 34**). At the age of two months these mice developed chronic diarrhea leading to a progressive wasting syndrome, frequently associated with anorectal prolapse. A marked dilation and thickening of the rectum and colon was found in advanced stages of disease and blood glucose levels were as low as 5 mM compared to 9-10 mM in control mice indicating insufficient food resorption (data not shown). Histological analysis of the inflamed colon in α 7.2 mice revealed elongated crypts, depletion of goblet cells, crypt abscesses and pronounced infiltration of inflammatory cells in the lamina propria (**Figure 35**).

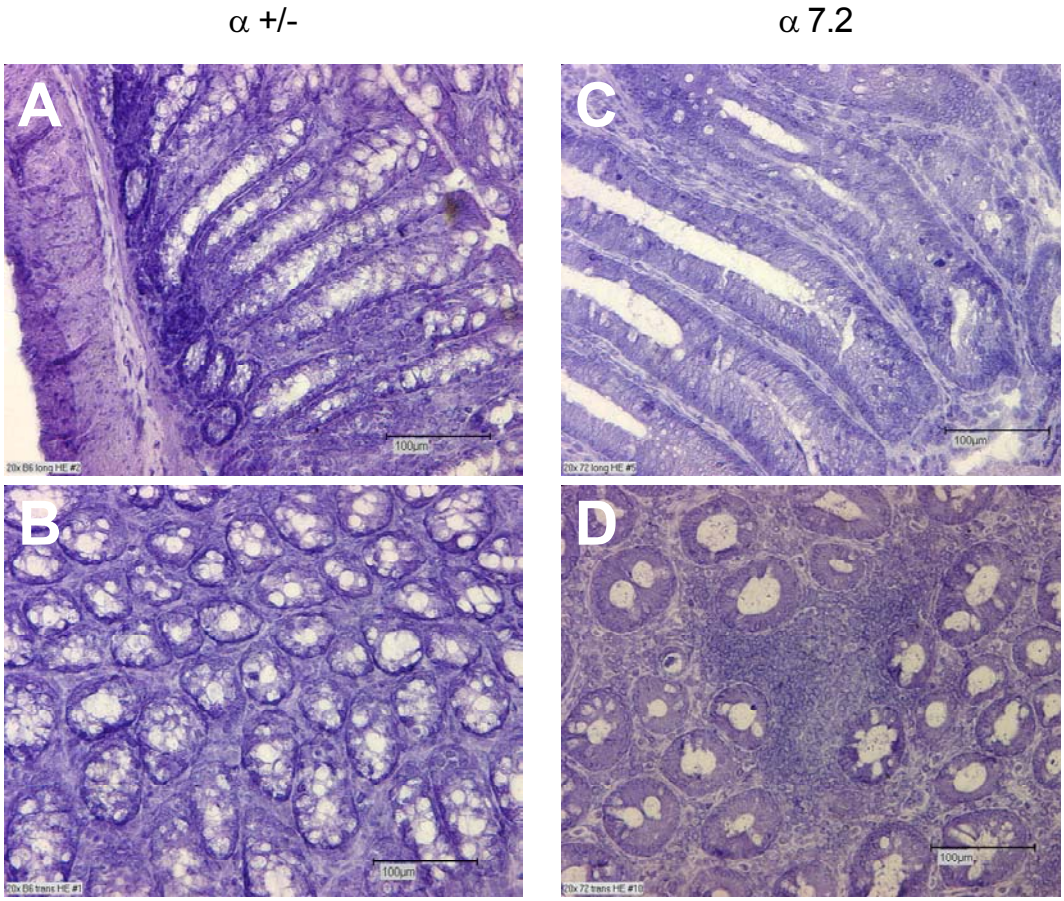

Figure 35. Histological analysis of IBD in α 7.2 mice. Histology of the colon was compared between 10 weeks old α+/- and α 7.2 mice. Hematoxylin-eosin staining of transverse and longitudinal sections of α +/- (**a,b**) and α 7.2 (**c,d**) littermates. Compared to control animals (**a,b**) elongated crypts, loss of goblet cells (large white cells) and massive cell infiltrates in the lamina propria are typical signs of pathology in α 7.2 mice (**c,d**). Original magnification x200, scale bars = 100µm.

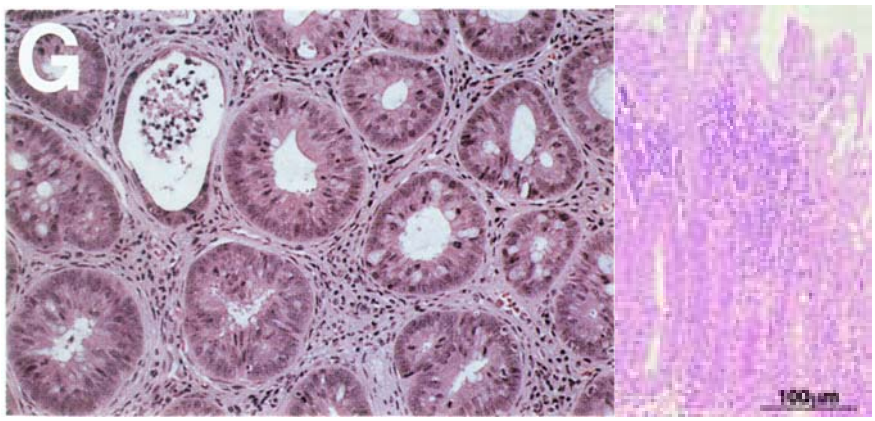

Figure 36. Published histology of IBD in α -/- mice. Hematoxylin-eosin stainings: taken from left (Mombaerts et al., 1993), right (Iijima et al., 1999)

Immunohistochemistry identified CD4+ T cells as the major constituents of granulomatous foci in the lamina propria (**Figure 37**). In contrast to control mice, large amounts of γδ T cells were found in the lamina propria and in the submucosa but not in the granulomatous foci. We cannot directly compare the pathology observed in α 7.2 mice to IBD in α -/- mice, because the α -/- mice did not develop symptoms of IBD in our animal facilities. For comparison, reported histology of IBD in 6-10 months old α -/- mice is shown in **Figure 36**. However, the IBD that manifested in α 7.2 mice at an age of 8-10 weeks was similar to the IBD described in aging animals (Mombaerts et al., 1993). This further underlines the capacity of non-pairing TCR α chain expression to significantly increase the size of the CD4+ TCR $\alpha^{-}\beta^{+}$ T cell population resulting in accelerated development of IBD in α 7.2 mice.

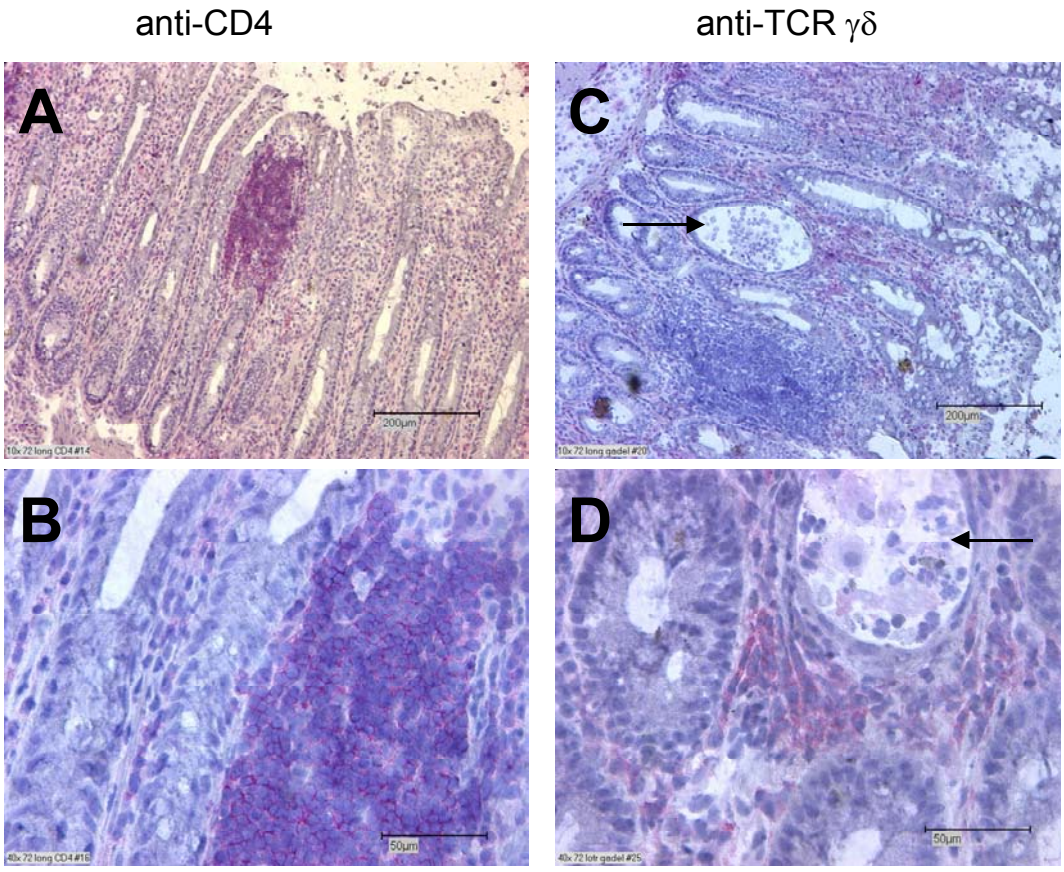

Figure 37. Analysis of T cells infiltrates. Frozen sections of the colon from 10 weeks old α 7.2 animals with IBD were immunohistochemically stained with anti CD4 mAb (**a,b**) or anti γδ TCR mAb (**c,d**). Focal granulomatous accumulation of CD4+ T cells (**a,b**) and scattered distribution of γδ T cells (**c,d**) is shown at low (x100, scale bars = 200µm) and high magnification (x400, scale bars = 50µm). (**c,d**) Arrow indicate crypt abscesses.

6.11 Stabilization of endogenous TCR β chains by non-pairing TCR α 7.2

How can expression of a non-functional TCR α chain cause elevated levels of CD4+ TCR $\alpha^{-}\beta^{+}$ T cells? To assess this question we examined the stability of TCR β chains in α -/- and α 7.2 thymocytes by pulse-chase labeling and subsequent immunoprecipitation of the TCR β chains. We found that newly synthesized TCR β chains are rapidly degraded in α -/- with a half-life ($t_{½}$) of 58 min compared to α +/- thymocytes with a $t_{½}$ of 75' min (**Figure 38**). Expression of α 7.2 in α -/- thymocytes rescued TCR β chains from rapid degradation and even prolonged the TCR β half-life relative to α +/- thymocytes ($t_{½}$ = 126'). We further found coimmunoprecipitation of the α 7.2 chain (**Figure 38A**). The apparent lower molecular weight of TCR α 7.2 is due to the lack of Asn-X-Ser/Thr N-glycosylation sites (Bennett et al., 1998). These results show that direct association of the transgenic α 7.2 chain with TCR β chains stabilizes the latter and protects them from degradation.

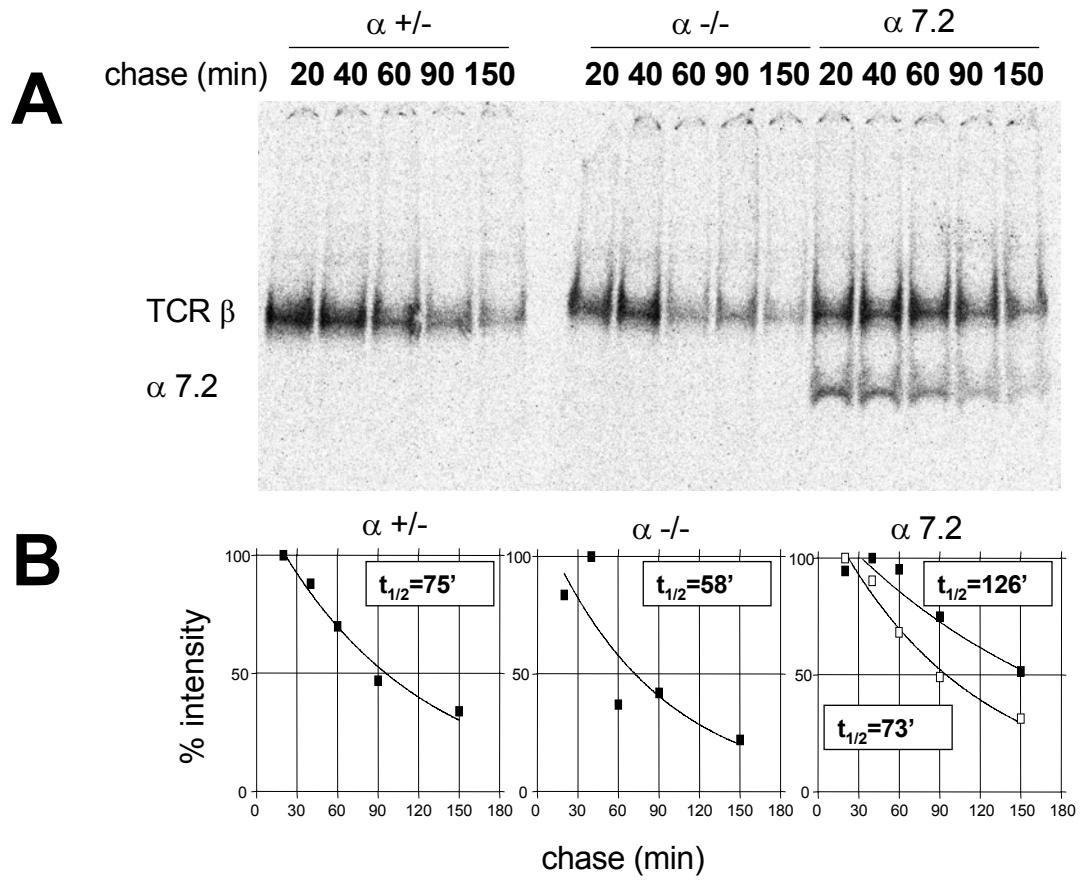

Figure 38. Transgenic TCR α 7.2 prolongs the half-life of TCR β. (**A**) Direct association and stabilization of TCR β chains by α 7.2. Thymocytes from α +/-, α -/- and α 7.2 mice were radiolabeled with [^{35}S]Met for 5 min and then chased in the presence of excess unlabeled Met for the indicated times. Lysates were immunoprecipitated with anti-TCR β mAb and analyzed by reducing SDS-PAGE. (**B**) Extended half-life of TCR β chains in α 7.2 mice. Nonlinear regression plot of labeled TCR β and of coimmunoprecipitated α 7.2 (□) quantified by densitometry. This experiment was performed twice with comparable results.